Journal of the Optical Society of America A
OPTICS, IMAGE SCIENCE, AND VISION

Goos–Hänchen and Imbert–Fedorov shifts of higher-order Laguerre–Gaussian beams reflected from a dielectric slab

KONSTANTIN N. PICHUGIN,[1] DMITRII N. MAKSIMOV,[1,2] AND ALMAS F. SADREEV[1,*]

[1]Kirensky Institute of Physics, Federal Research Center KSC SB RAS, 660036 Krasnoyarsk, Russia
[2]Reshetnev Siberian State University of Science and Technology, 660037 Krasnoyarsk, Russia
*Corresponding author: almas@tnp.krasn.ru

Received 4 April 2018; revised 30 May 2018; accepted 14 June 2018; posted 14 June 2018 (Doc. ID 327598); published 12 July 2018

We consider reflection of the Laguerre–Gaussian light beams by a dielectric slab. In view of the unified operator approach, the higher-order Laguerre–Gaussian beams represent a parametric family with the transverse beam profile given by an arbitrary generating parameter. Relying on the Fourier expansion in the focal plane of the beam, we compute the Goos–Hänchen and the Imbert–Fedorov shifts for light beams with non-zero order and azimuthal index. It is demonstrated that both shifts exhibit resonant behavior as functions of the angle of incidence due to the interference between the waves reflected from the upper and lower interfaces. The centroid shifts strongly depend on the order and azimuthal index of the beam. Most interestingly, it is found that the generating parameter of the higher-order beam families strongly affects the shifts. Thus, reshaping of the incident wavefront with fixed order and azimuthal index changes the linear Goos–Hänchen shift up to one half of the beam radius, both negative and positive.

OCIS codes: (240.0240) Optics at surfaces; (260.0260) Physical optics; (290.0290) Scattering.

https://doi.org/10.1364/JOSAA.35.001324

1. INTRODUCTION

It is well known that a bounded beam upon reflection and transmission on a planar interface differs in propagation with plane waves due to diffraction corrections. This may manifest as beam shifts with respect to the geometric optics prediction for reflection or refraction. The dominant shifts are the Goos–Hänchen (GH) shift in which the beam is displaced parallel to the plane of incidence [1], and the Imbert–Fedorov (IF) shift in which the shift is perpendicular [2]. Moreover, it has been shown that each of these two beam shifts can be separated into a spatial and an angular shift. The main distinction between spatial and angular shifts is the enhancement of the latter with the propagation of the beam [3].

The Laguerre–Gaussian (LG) beam is specified by two indices. The azimuthal index l up to a normalization constant corresponds to orbital angular momentum (OAM) of the beam, while the radial index p is the order of the associated Laguerre polynomial entering the expression for the beam profile. Throughout the paper, we will refer to p as the order of the LG beam. The effect of OAM on GH and IF shifts was considered for reflection of the LG beam from an interface [4–17]. These studies revealed the relation of the IF shift to the magnitude OAM and the dual nature of spatial and angular shifts in optical beam reflection, as well as the coupling of IF and GH shifts for OAM beams. In the present paper, we extend these studies to reflection of higher-order LG beams from a dielectric slab, as sketched in Fig. 1. In what follows, the term "higher-order" LG beam shall be applied to all beams with radial index $p > 0$, to stress that it is the radial dependence of the beam profile that plays the crucial role in the interference effects. The presence of two interfaces of the slab brings in a resonant behavior of the GH and IF shifts, as was demonstrated for the reflection of Gaussian beams [18–20] and LG beams [21] by a dielectric slab. The brightest effect of interference of reflected and transmitted beams is a reshaping of the beam profile [21,22].

Following Enderlein and Pampaloni, we define LG beams via the unified operator approach [23]. In that approach, the higher-order LG beam modes represent a parametric family with the transverse beam profile controlled by an arbitrary generating parameter that allows varying the profile with fixed order and azimuthal index. Structured light plays an important role in modern science and technology [24]. Only recently, however, have we witnessed a surge of interest to higher-order LG beams [25–30], which have applications to interferometry [31] and harmonics generation [32]. Currently, the higher-order LG beams can be experimentally generated with a variety of methods, including the use of spatial light modulators [33],

fork-holograms [31,34], fork-gratings [35], spiral phase plates [36], and modal q-plates [37]. Here we address the centroid shifts of the higher-order LG beams in dependence on the transverse beam profile as well as the order and azimuthal index of the beam.

2. LAGUERRE–GAUSSIAN BEAMS

In the framework of the unified operator approach [23], the LG mode of arbitrary order p and azimuthal index l is derived by acting with differential operators $\widehat{\mathcal{L}}, \widehat{\mathcal{L}}^*$ on the Fourier representation of the fundamental Gaussian beam:

$$E(\mathbf{r}) = \int_{-\infty}^{+\infty} \frac{\mathrm{d}k_x \mathrm{d}k_y}{(2\pi)^2} \widehat{\mathcal{L}}^p (\widehat{\mathcal{L}}^*)^{p+l} e^S, \tag{1}$$

where

$$e^S = e^{ik_x x + ik_y x + ikz - i(k_x^2+k_y^2)z/2k} A_0, \tag{2}$$

where k_x, k_y are the wave vector components in the Fourier plane of the beam $x0y$, k is the wave number, z is the axial coordinate of the beam in Fig. 1, and, finally, the Fourier amplitude of the fundamental Gaussian mode is given by

$$A_0 = e^{-w_0^2(k_x^2+k_y^2)/4}. \tag{3}$$

The differential operator in Eq. (1) is defined in the following manner:

$$\widehat{\mathcal{L}} = i(k_x + ik_y) + \frac{1}{u}\left(\frac{\partial}{\partial k_x} + i\frac{\partial}{\partial k_x}\right), \tag{4}$$

with u as an arbitrary complex valued parameter. Eq. (1) can be rewritten in a more convenient form:

$$E(\mathbf{r}) = \int_{-\infty}^{+\infty} \frac{\mathrm{d}k_x \mathrm{d}k_y}{(2\pi)^2} A_p^l(k_x, k_y) e^{ik_x x + ik_y x + ikz - i(k_x^2+k_y^2)z/2k}, \tag{5}$$

where $A_p^l(k_x, k_y)$ is the Fourier amplitude of the LG mode of arbitrary order and azimuthal index (see Appendix A):

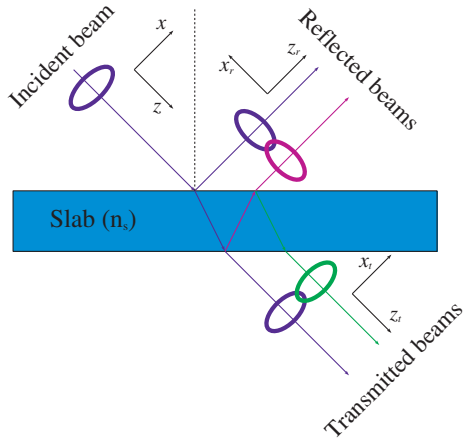

Fig. 1. LG beam reflected and refracted by a dielectric slab with thickness d and refractive index n_s. The coordinate axes are shown in the plane of incidence. For all coordinate systems, the y axis is perpendicular to the plane of the plot.

$$A_p^l(k_x, k_y) = i^{p+l} p! \left(\frac{-2}{u}\right)^p (k_x - ik_y)^l \times L_p^l\left[\frac{iu(k_x^2+k_y^2)}{2}\right] e^{-w_0^2(k_x^2+k_y^2)/4}, \tag{6}$$

where $L_p^l(x)$ is the associated Laguerre polynomial. In the case of $u = -iw_0^2$, the latter formula coincides with the Fourier representation of the regular LG beams [38]. The electric field amplitude of the paraxial LG beams can be found as [23]

$$E(\mathbf{r}) = (2f)^{2p+l}(-1)^{p+l} p! g^p (\omega_2 g)^l L_p^l(g\omega_1\omega_2) E_0(\mathbf{r}), \tag{7}$$

where

$$\omega_1 = x + iy, \qquad \omega_2 = x - iy, \tag{8}$$

$$f = 1 + \frac{i}{u}\left(\frac{iz}{k} + \frac{w_0^2}{2}\right), \tag{9}$$

$$g = \frac{2u}{(w_0^2 + 2iz/k)[2u + i(w_0^2 + 2iz/k)]}, \tag{10}$$

and $E_0(\mathbf{r})$ is the field profile of the fundamental Gaussian mode:

$$E_0(\mathbf{r}) = \frac{1}{\pi}\frac{1}{(w_0^2 + 2iz/k)} e^{ikz - i(k_x^2+k_y^2)z/2k - \frac{x^2+y^2}{(w_0^2+2iz/k)}}. \tag{11}$$

In Fig. 2, we plot the profiles of higher-order $p = 1, 2$ LG modes for three different values of u. One can see in Fig. 2 that the generating parameter u strongly affects the profile of the LG modes with the same p and l.

3. BEAM SHIFTS

Let us consider LG beams reflected from a planar structure. The profile of the reflected beam can be found in the following form:

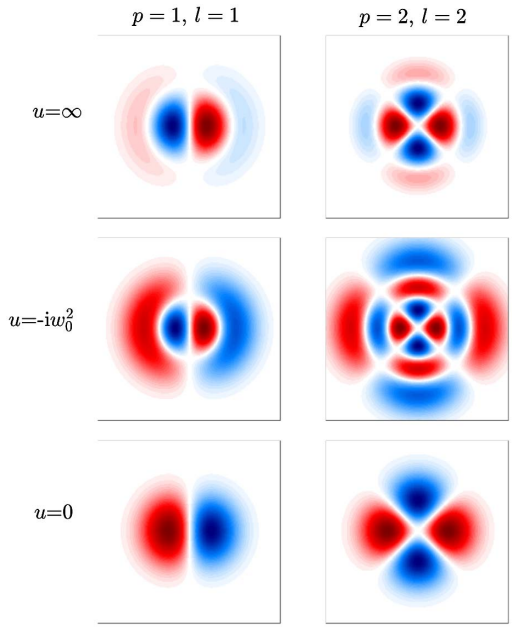

Fig. 2. Beam profiles as the real part of Eq. (7) in the Fourier plane.

$$E_r(\mathbf{r}_r) = \int_{-\infty}^{+\infty} \frac{\mathrm{d}k_x \mathrm{d}k_y}{(2\pi)^2} A_p^l(k_x, k_y) r(k_x, k_y) e^{-ik_x x_r + ik_y y_r + i\psi_r}, \tag{12}$$

where $r(k_x, k_y)$ are the reflection amplitudes specified by each individual plane wave propagation direction, and ψ_r is the phase acquired by the plane wave on its way from the focal plane to the reflection interface, and then from the reflection interface to the observation point. Notice that the phase ψ_r is defined in the coordinates of the reflected beam $\{x_r, y_r, z_r\}$, where the z_r axis is aligned with the reflected beam propagation direction reconstructed by ray tracing. Such a coordinate system can be easily set by the mirror reflection of the incident beam coordinate system basis vectors with respect to the plane of the interface. In the paraxial approximation, the phase is written as

$$\psi_r = kz_r - (k_x^2 + k_y^2) z_r / 2k + \psi_0(k_x, k_y), \tag{13}$$

where $\psi_0(k_x, k_y)$ is the phase acquired by a plane wave on its wave from the focal plane to the interface. This phase can be found from the distance z_0 between the focal plane and the interface along the beam axis:

$$\psi_0(k_x, k_y) = kz_0 - (k_x^2 + k_y^2) z_0 / 2k. \tag{14}$$

Now we assume that the definition of the reflection amplitudes $r(k_x, k_y)$ is consistent with the new coordinate frame. The reflectance of the beam is given by

$$R = \int_{-\infty}^{+\infty} \mathrm{d}x_r \mathrm{d}y_r |E_r(\mathbf{r})|^2. \tag{15}$$

Substituting Eqs. (12)–(15) and using the Fourier expansion of the Dirac delta function

$$\delta(k) = \frac{1}{2\pi} \int_{-\infty}^{+\infty} \mathrm{d}k e^{ixk}, \tag{16}$$

we find

$$R = \frac{1}{(2\pi)^2} \int_{-\infty}^{+\infty} \int_{-\infty}^{+\infty} \mathrm{d}k_x \mathrm{d}k_y |A_r(k_x, k_y)|^2, \tag{17}$$

where

$$A_r(k_x, k_y) = r(k_x, k_y) A_p^l(k_x, k_y). \tag{18}$$

Now assume that the y and y_r axes are orthogonal to the plane of incidence, i.e., to the plane containing the incident wave vector and the normal to the interface. Then the lateral shift of the reflected beam is found as

$$\langle x_r \rangle = \frac{1}{R} \int_{-\infty}^{+\infty} \mathrm{d}x_r \mathrm{d}y_r x_r |E_r(\mathbf{r})|^2. \tag{19}$$

Integrating by parts and using Eq. (16), we find the following expression for the lateral shift:

$$\langle x_r \rangle = \frac{-i}{R} \int_{-\infty}^{+\infty} \frac{\mathrm{d}k_x \mathrm{d}k_y}{(2\pi)^2} \times \left[\frac{\partial A_r^*(k_x, k_y)}{\partial k_x} + ik_x \frac{z_0 + z_r}{k} A_r^*(k_x, k_y) \right] A_r(k_x, k_y). \tag{20}$$

One can show that $\langle x_r \rangle$ can be split into two summands. The first one, independent of z_r, defines the GH shift:

$$S_{\mathrm{GH}} = \frac{1}{R} \int_{-\infty}^{+\infty} \frac{\mathrm{d}k_x \mathrm{d}k_y}{(2\pi)^2} \times \left[\mathrm{Im}\left\{ \frac{\partial A_r^*(k_x, k_y)}{\partial k_x} A_r(k_x, k_y) \right\} + \frac{k_x z_0}{k} |A_r(k_x, k_y)|^2 \right]. \tag{21}$$

At the same time, the second term defines the angular GH shift:

$$S_{\mathrm{GHA}} = \frac{1}{R} \int_{-\infty}^{+\infty} \frac{\mathrm{d}k_x \mathrm{d}k_y}{(2\pi)^2} \frac{z_r k_x}{k} |A_r(k_x, k_y)|^2. \tag{22}$$

The angular GH shift can be more conveniently described by the angular deviation from the ray optics prediction for the ray trajectory:

$$\alpha_{\mathrm{GH}} = \arcsin\left(\frac{S_{\mathrm{GHA}}}{z_r} \right). \tag{23}$$

Both linear S_{IF} and angular S_{IFA} IF shifts are defined in the same manner by replacing x_r with y_r:

$$S_{\mathrm{IF}} = \frac{-1}{R} \int_{-\infty}^{+\infty} \frac{\mathrm{d}k_x \mathrm{d}k_y}{(2\pi)^2} \times \left[\mathrm{Im}\left\{ \frac{\partial A_r^*(k_x, k_y)}{\partial k_y} A_r(k_x, k_y) \right\} + \frac{k_y z_0}{k} |A_r(k_x, k_y)|^2 \right], \tag{24}$$

and

$$S_{\mathrm{IFA}} = \frac{-1}{R} \int_{-\infty}^{+\infty} \frac{\mathrm{d}k_x \mathrm{d}k_y}{(2\pi)^2} \frac{z_r k_y}{k} |A_r(k_x, k_y)|^2. \tag{25}$$

4. NUMERICAL RESULTS

As a numerical example, we consider an infinite dielectric slab of thickness d and refractive index n_s embedded into a medium with refractive index $n = 1$ (vacuum), as shown in Fig. 1. Following Okuda and Sasada [39], we do not consider cross-polarization effects [40,41], choosing the incident beam with a small paraxial parameter $2\pi / k w_0 = 0.01$. The reflection coefficient of the s-polarized plane wave through the slab can be written as [42]

$$r = r_s \left(1 - \frac{\exp(2id\overline{k}_Z) t_s \tilde{t}_s}{1 - (r_s)^2 \exp(2id\overline{k}_Z)} \right), \tag{26}$$

where $r_s, t_s, \tilde{t}_s$ are Fresnel coefficients:

$$r_s = \frac{k_Z - \overline{k}_Z}{k_Z + \overline{k}_Z}, \tag{27}$$

$$t_s = 2 \frac{k_Z}{k_Z + \overline{k}_Z}, \tag{28}$$

$$\tilde{t}_s = 2 \frac{\overline{k}_Z}{k_Z + \overline{k}_Z}, \tag{29}$$

with $k_Z = \sqrt{k^2 - k_X^2 - k_Y^2}$, $\overline{k}_Z = \sqrt{(kn_s)^2 - k_X^2 - k_Y^2}$, and k_X, k_Y as the components of the vacuum wave vector in the fixed reference frame $\{X, Y, Z\}$ of the slab, as shown in

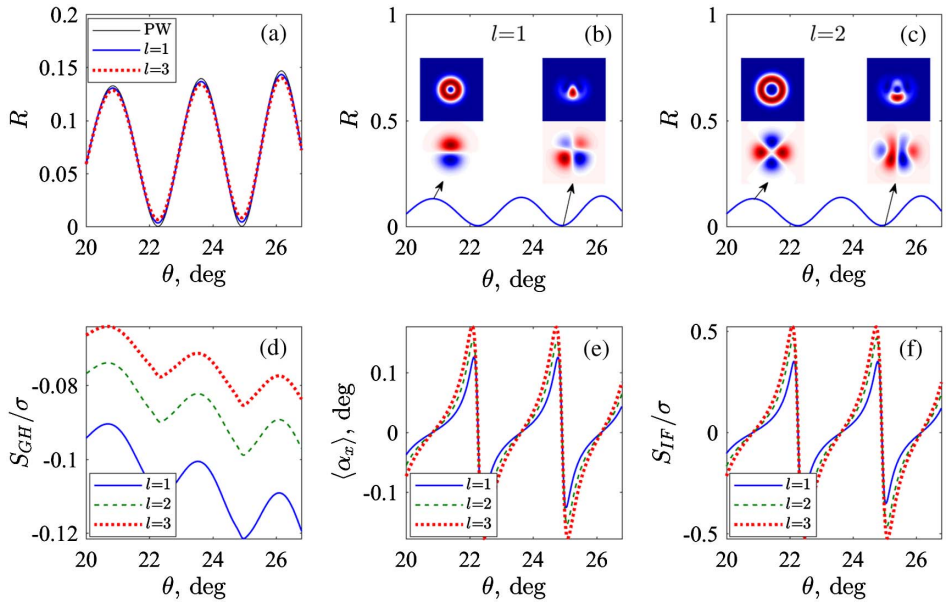

Fig. 3. (a) Reflectance of the LG beams with different azimuthal index l from a dielectric slab of thickness $d = 40\lambda_0$ and refractive index $n = \sqrt{2}$ versus the angle of incidence of the beam. The reflectance of a plane wave (PW) is shown for comparison by a thin black line. (b)-(c) Profiles of reflected beams at different angles of incidence for LG beams with $p = 0$ and $l = 1, 2$, respectively, at the minima and maxima of reflectance R. Real part of the scattered beam profile, lower inset; intensity, upper inset. (d) GH, (e) angular GH, and (f) IF shifts for different values of l.

Fig. 1. Thus, to be used in Eqs. (18) and (26), they should be transformed to the incident beam coordinates $\{x, y, z\}$. Using Eqs. (18), (21), (23), and (24) with the reflection coefficient Eq. (26) and Fourier amplitude Eq. (6), we computed the centroid shifts of s-polarized beams focused on the upper interface as dependent on the angle of incidence θ, as well as on the order and azimuthal index of the beam. The beams wavelength was taken $\lambda_0 = 0.6328$ μm, with the width of the slab $d = 40\lambda_0$, and $w_0 = 100\lambda_0$.

In Fig. 3, we show the reflection coefficients and centroid shifts of zero-order ($p = 0$) LG beams with a different azimuthal index versus the angle of incidence. The GH and IF shifts are normalized to the spatial extension of the incident beam in its waist:

$$\sigma^2 = \int_{-\infty}^{+\infty} \mathrm{d}x\mathrm{d}y(x^2 + y^2)|E(x, y, z_0)|^2, \qquad (30)$$

where $z_0 = 0$ is the point of intersection of the beam axis with the upper interface (see Fig. 1) on which the beam is focused. As seen in Fig. 3(a), the reflectance of the OAM beams exhibits a resonant behavior typical for two-interface Fabry–Perot structures closely following the reflectance of a plane wave, Eq. (26). One can see that the azimuthal index does not strongly affect the reflectance. The obvious effect is disappearance of the reflectance zeros. However, as shown in Figs. 3(d)–3(f), the IF and GH shifts ratio to the beam radius depends on l. The angular IF shift is zero, since the integrand in Eq. (25) is an antisymmetric function.

As seen in Fig. 1, in reflection of a LG beam from the dielectric slab, there is interference of many optical paths with waves bouncing between the interfaces. One can expect that the superposed beam has a complicated structure in its Fourier plane. In Figs. 3(b) and 3(c), we show the reflected beam profiles for different azimuthal indices at those angles of incidence that correspond to the minima and maxima of reflectance. One can see in Figs. 3(b) and 3(c) that the beam profiles are strongly distorted at the minima of the reflectance where the contribution to the Fourier representation critically depends on the propagation direction of a Fourier component. That qualitatively explains the largest centroid shifts in the vicinity of the plane wave reflectance zeros. At the same time, the oscillatory behavior of the centroid shifts in Figs. 3(d)–3(f) can be understood from the oscillatory behavior of the reflection coefficient, Eq. (26).

In Fig. 4, we show the centroid shift of higher-order LG beams. One can see in Figs. 4(a) and 4(b) that the magnitude of both the GH and IF shifts is strongly affected by the generating parameter u. In Figs. 4(c)–4(e), we demonstrate the variation range of the centroid shifts against the angle of incidence with u changing across the whole complex plane. The dependence of the centroid shifts on the angle of incidence demonstrates an oscillatory behavior induced by the oscillatory behavior of Eq. (26). As before, the strongest shifts are observed in the vicinity of the reflectance minima. Most remarkable, though, is that the variation of u significantly enhances the GH shift (up to five times) in comparison to the regular LG beams. In addition, the sign of the GH shift can be changed by tuning the generating parameter u. The effect of u on the centroid shifts can be qualitatively understood in Fig. 2, where one can see a significant change of the beam profile under variation of u.

5. CONCLUSION

Earlier, Bliokh *et al.* [8] predicted vortex-induced GH shift related to the angular IF shift for reflection of the LG beam from

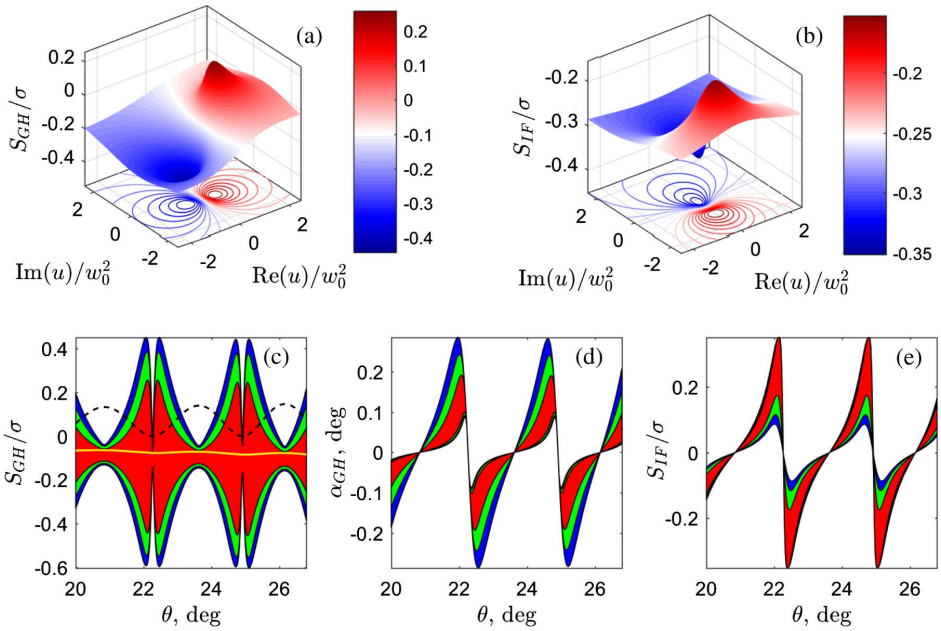

Fig. 4. (a) GH and (b) IF shifts for LG beam with $p = 1, l = 1$ at the incidence angle $\theta = 22.125$ deg. Range of (d) GH, (e) angular GH, and (f) IF shifts against the angle of incidence for $l = 1$ and different values of the beam order p; $p = 1$, red-filled area; $p = 2$, green-filled area; $p = 3$, blue-filled area. The GH shift for the regular LG beam with $p = 1$ is shown in (c) by a yellow line. The reflectance of the beam with $p = 1$ is shown in (c) by a dashed black line. The other optogeometric parameters are the same as in Fig. 3.

an interface separating two dielectric media. Similar phenomena take place in reflection from a dielectric slab. As one can expect, the GH and IF shifts depend on the azimuthal index. It is clear that the sign of the IF shifts depends on the sign of l. The presence of two interfaces of the slab brings in a resonant behavior of the GH and IF shifts. That type of behavior was not observed in the earlier studies [21], because the beam divergence far exceeded the distance between the resonant peaks in Eq. (26). Scattering of the incident LG beam from a dielectric slab gives rise to interference between reflected LG beams (Fig. 1), which, in turn, results in restructuring of reflected light, as shown in Fig. 3.

Following Enderlein and Pampaloni, we considered LG beams within the unified operator approach [23]. In that approach, higher-order LG beams represent a parametric family with the transverse beam profile given by an arbitrary generating parameter u, which allows varying the profile of the beam with fixed order and azimuthal index. As a result, the generating parameter of higher-order beam families strongly affects the centroid shifts. Thus, reshaping of the incident wavefront with fixed order p and azimuthal index l changes the linear GH shift up to one half of the beam radius, both negative and positive, as seen in Fig. 4. We speculate that introducing the parametric family of the higher-order LG beams can bring a new dimension to engineering interference effects in propagation and scattering of structured light.

APPENDIX A: FOURIER AMPLITUDE OF LG BEAMS

After a coordinate change,

$$k_1 = k_x + ik_y, \qquad k_2 = k_x - ik_y, \tag{A1}$$

Eq. (1) is written as

$$E(\mathbf{r}) = \int_{-\infty}^{+\infty} \frac{\mathrm{d}k_1 \mathrm{d}k_1}{2(2\pi)^2} \left[ik_1 + \frac{2}{u}\frac{\partial}{\partial k_2}\right]^p \left[ik_2 + \frac{2}{u}\frac{\partial}{\partial k_1}\right]^{p+l} e^S. \tag{A2}$$

Now let us write

$$e^S = VG, \qquad G = e^{-iuk_1k_2/2}, \qquad V = e^{S+iuk_1k_2/2}, \tag{A3}$$

then Eq. (A2) is again simplified as

$$E(\mathbf{r}) = \left(\frac{2}{u}\right)^{2p+l} \int_{-\infty}^{+\infty} \frac{\mathrm{d}k_1 \mathrm{d}k_1}{2(2\pi)^2} G \frac{\partial^p}{\partial^p k_2} \frac{\partial^{p+l}}{\partial^{p+l} k_1} V. \tag{A4}$$

Integrating by parts, we have

$$E(\mathbf{r}) = (-1)^l \left(\frac{2}{u}\right)^{2p+l} \int_{-\infty}^{+\infty} \frac{\mathrm{d}k_1 \mathrm{d}k_1}{2(2\pi)^2} V \frac{\partial^p}{\partial^p k_2} \frac{\partial^{p+l}}{\partial^{p+l} k_1} G. \tag{A5}$$

Next, by recollecting the definition of the associated Laguerre polynomials,

$$L_p^l(r) = \frac{e^r r^{-l}}{p!} \frac{d^p}{dr^p}(e^{-r} r^{p+l}), \tag{A6}$$

we have

$$E(\mathbf{r}) = (-1)^p p! \left(\frac{2}{u}\right)^{2p+l} \int_{-\infty}^{+\infty} \frac{\mathrm{d}k_1 \mathrm{d}k_1}{2(2\pi)^2} \times \left(\frac{iu}{2}\right)^p \left(\frac{iuk_2}{2}\right)^l L_p^l\left(\frac{iuk_1k_2}{2}\right) e^S. \tag{A7}$$

Finally, returning to the initial coordinates k_x, k_y, we have Eqs. (5) and (6).

Funding. Russian Foundation for Basic Research (RFBR) (17-52-45072).

Acknowledgment. We acknowledge discussions with Jayachandra Bingi.

REFERENCES

1. F. Goos and H. Hänchen, "Ein neuer und fundamentaler versuch zur totalreflexion," Ann. Phys. **436**, 333–346 (1947).
2. C. Imbert, "Calculation and experimental proof of the transverse shift induced by total internal reflection of a circularly polarized light beam," Phys. Rev. D **5**, 787–796 (1972).
3. A. Aiello and J. P. Woerdman, "Role of beam propagation in Goos-Hänchen and Imbert-Fedorov shifts," Opt. Lett. **33**, 1437–1439 (2008).
4. L. Allen, M. W. Beijersbergen, R. J. C. Spreeuw, and J. P. Woerdman, "Orbital angular momentum of light and the transformation of Laguerre-Gaussian laser modes," Phys. Rev. A **45**, 8185–8189 (1992).
5. V. Fedoseyev, "Spin-independent transverse shift of the centre of gravity of a reflected and of a refracted light beam," Opt. Commun. **193**, 9–18 (2001).
6. A. Bekshaev, "Method of light beam orbital angular momentum evaluation by means of space-angle intensity moments," Ukr. J. Phys. Opt. **3**, 249–257 (2002).
7. V. G. Fedoseyev, "Transformation of the orbital angular momentum at the reflection and transmission of a light beam on a plane interface," J. Phys. A **41**, 505202 (2008).
8. K. Y. Bliokh, I. V. Shadrivov, and Y. S. Kivshar, "Goos-Hänchen and Imbert-Fedorov shifts of polarized vortex beams," Opt. Lett. **34**, 389–391 (2009).
9. A. Y. Bekshaev, "Oblique section of a paraxial light beam: criteria for azimuthal energy flow and orbital angular momentum," J. Opt. A **11**, 094003 (2009).
10. M. Merano, A. Aiello, M. P. van Exter, and J. P. Woerdman, "Observing angular deviations in the specular reflection of a light beam," Nat. Photonics **3**, 337–340 (2009).
11. M. Merano, N. Hermosa, J. P. Woerdman, and A. Aiello, "How orbital angular momentum affects beam shifts in optical reflection," Phys. Rev. A **82**, 023817 (2010).
12. A. Aiello, "Goos-Hänchen and Imbert-Fedorov shifts: a novel perspective," New J. Phys. **14**, 013058 (2012).
13. G. Jayaswal, G. Mistura, and M. Merano, "Weak measurement of the Goos-Hänchen shift," Opt. Lett. **38**, 1232–1234 (2013).
14. K. Y. Bliokh and A. Aiello, "Goos-Hänchen and Imbert-Fedorov beam shifts: an overview," J. Opt. **15**, 014001 (2013).
15. B. R. Horowitz and T. Tamir, "Lateral displacement of a light beam at a dielectric interface," J. Opt. Soc. Am. **61**, 586–594 (1971).
16. H. Okuda and H. Sasada, "Huge transverse deformation in nonspecular reflection of a light beam possessing orbital angular momentum near critical incidence," Opt. Express **14**, 8393–8402 (2006).
17. M. A. Berbel, A. Cunillera, and R. Martínez-Herrero, "Goos-Hänchen and Imbert-Fedorov shifts: relation with the irradiance moments of a beam," J. Opt. Soc. Am. A **35**, 286–292 (2018).
18. C.-F. Li, "Negative lateral shift of a light beam transmitted through a dielectric slab and interaction of boundary effects," Phys. Rev. Lett. **91**, 133903 (2003).
19. L.-G. Wang, H. Chen, and S.-Y. Zhu, "Large negative Goos-Hänchen shift from a weakly absorbing dielectric slab," Opt. Lett. **30**, 2936–2938 (2005).
20. J. Wen, J. Zhang, L.-G. Wang, and S.-Y. Zhu, "Goos-Hänchen shifts in an epsilon-near-zero slab," J. Opt. Soc. Am. B **34**, 2310–2316 (2017).
21. H. Li, F. Honary, Z. Wu, and L. Bai, "Reflection and transmission of Laguerre-Gaussian beams in a dielectric slab," J. Quant. Spectrosc. Radiat. Transfer **195**, 35–43 (2017).
22. D. A. Bykov, L. L. Doskolovich, A. A. Morozov, V. V. Podlipnov, E. A. Bezus, P. Verma, and V. A. Soifer, "Spatial differentiation of three-dimensional optical beams using guided-mode resonant grating," preprint arXiv:1803.02058 (2018).
23. J. Enderlein and F. Pampaloni, "Unified operator approach for deriving Hermite-Gaussian and Laguerre-Gaussian laser modes," J. Opt. Soc. Am. A **21**, 1553–1558 (2004).
24. H. Rubinsztein-Dunlop, A. Forbes, M. V. Berry, M. R. Dennis, D. L. Andrews, M. Mansuripur, C. Denz, C. Alpmann, P. Banzer, T. Bauer, E. Karimi, L. Marrucci, M. Padgett, M. Ritsch-Marte, N. M. Litchinitser, N. P. Bigelow, C. Rosales-Guzmán, A. Belmonte, J. P. Torres, T. W. Neely, M. Baker, R. Gordon, A. B. Stilgoe, J. Romero, A. G. White, R. Fickler, A. E. Willner, G. Xie, B. McMorran, and A. M. Weiner, "Roadmap on structured light," J. Opt. **19**, 013001 (2016).
25. E. Karimi, R. W. Boyd, P. de la Hoz, H. de Guise, J. Řeháček, Z. Hradil, A. Aiello, G. Leuchs, and L. L. Sánchez-Soto, "Radial quantum number of Laguerre-Gauss modes," Phys. Rev. A **89**, 063813 (2014).
26. W. N. Plick and M. Krenn, "Physical meaning of the radial index of Laguerre-Gauss beams," Phys. Rev. A **92**, 063841 (2015).
27. J. Mendoza-Hernández, M. L. Arroyo-Carrasco, M. D. Iturbe-Castillo, and S. Chávez-Cerda, "Laguerre-Gauss beams versus Bessel beams showdown: peer comparison," Opt. Lett. **40**, 3739–3742 (2015).
28. G. Vallone, G. Parisi, F. Spinello, E. Mari, F. Tamburini, and P. Villoresi, "General theorem on the divergence of vortex beams," Phys. Rev. A **94**, 023802 (2016).
29. A. A. Kovalev, V. V. Kotlyar, and A. P. Porfirev, "Asymmetric Laguerre-Gaussian beams," Phys. Rev. A **93**, 063858 (2016).
30. D. A. Savelyev, S. N. Khonina, and I. Golub, *Tight Focusing of Higher Orders Laguerre-Gaussian Modes* (American Institute of Physics, 2016).
31. M. Granata, C. Buy, R. Ward, and M. Barsuglia, "Higher-order Laguerre-Gauss mode generation and interferometry for gravitational wave detectors," Phys. Rev. Lett. **105**, 231102 (2010).
32. R. Géneaux, C. Chappuis, T. Auguste, S. Beaulieu, T. T. Gorman, F. Lepetit, L. F. DiMauro, and T. Ruchon, "Radial index of Laguerre-Gaussian modes in high-order-harmonic generation," Phys. Rev. A **95**, 051801 (2017).
33. N. Matsumoto, T. Ando, T. Inoue, Y. Ohtake, N. Fukuchi, and T. Hara, "Generation of high-quality higher-order Laguerre-Gaussian beams using liquid-crystal-on-silicon spatial light modulators," J. Opt. Soc. Am. A **25**, 1642–1651 (2008).
34. J. Arlt, K. Dholakia, L. Allen, and M. J. Padgett, "The production of multiringed Laguerre-Gaussian modes by computer-generated holograms," J. Mod. Opt. **45**, 1231–1237 (1998).
35. P. Chen, B.-Y. Wei, W. Ji, S.-J. Ge, W. Hu, F. Xu, V. Chigrinov, and Y.-Q. Lu, "Arbitrary and reconfigurable optical vortex generation: a high-efficiency technique using director-varying liquid crystal fork gratings," Photon. Res. **3**, 133–139 (2015).
36. G. Ruffato, M. Massari, and F. Romanato, "Generation of high-order Laguerre-Gaussian modes by means of spiral phase plates," Opt. Lett. **39**, 5094–5097 (2014).
37. M. Rafayelyan and E. Brasselet, "Laguerre-Gaussian modal q-plates," Opt. Lett. **42**, 1966–1969 (2017).
38. J. Ou, Y. Jiang, J. Zhang, and Y. He, "Reflection of Laguerre-Gaussian beams carrying orbital angular momentum: a full Taylor expanded solution," J. Opt. Soc. Am. A **30**, 2561–2571 (2013).
39. H. Okuda and H. Sasada, "Significant deformations and propagation variations of Laguerre-Gaussian beams reflected and transmitted at a dielectric interface," J. Opt. Soc. Am. A **25**, 881–890 (2008).
40. A. Köházi-Kis, "Cross-polarization effects of light beams at interfaces of isotropic media," Opt. Commun. **253**, 28–37 (2005).
41. K. Y. Bliokh and Y. P. Bliokh, "Polarization, transverse shifts, and angular momentum conservation laws in partial reflection and refraction of an electromagnetic wave packet," Phys. Rev. E **75**, 066609 (2007).
42. M. Born and E. Wolf, *Principles of Optics: Electromagnetic Theory of Propagation, Interference and Diffraction of Light* (Elsevier, 2013).